

# Improving performance of contour integral-based nonlinear eigensolvers with infinite GMRES

Yuqi Liu<sup>1</sup>, Jose E. Roman<sup>2</sup>, and Meiyue Shao<sup>3,4</sup>

<sup>1</sup>*School of Mathematical Sciences, Fudan University, Shanghai 200433, China*

<sup>2</sup>*D. Sistemes Informàtics i Computació, Universitat Politècnica de València, Camí de Vera s/n, 46022 València, Spain*

<sup>3</sup>*School of Data Science, Fudan University, Shanghai 200433, China*

<sup>4</sup>*Shanghai Key Laboratory for Contemporary Applied Mathematics, Fudan University, Shanghai 200433, China*

January 28, 2025

## Abstract

In this work, the infinite GMRES algorithm, recently proposed by Correnty *et al.*, is employed in contour integral-based nonlinear eigensolvers, avoiding the computation of costly factorizations at each quadrature node to solve the linear systems efficiently. Several techniques are applied to make the infinite GMRES memory-friendly, computationally efficient, and numerically stable in practice. More specifically, we analyze the relationship between polynomial eigenvalue problems and their scaled linearizations, and provide a novel weighting strategy which can significantly accelerate the convergence of infinite GMRES in this particular context. We also adopt the technique of TOAR to infinite GMRES to reduce the memory footprint. Theoretical analysis and numerical experiments are provided to illustrate the efficiency of the proposed algorithm.

**Keywords:** Krylov methods, infinite Arnoldi, nonlinear eigenvalue problem, contour integration, companion linearization.

**AMS subject classifications (2020).** 65F10, 65F15, 65F50

## 1 Introduction

By nonlinear eigenvalue problem (NEP), we refer to

$$T(\lambda)v = 0, \quad v \in \mathbb{C}^n \setminus \{0\}, \quad \lambda \in \Omega, \quad (1)$$

where  $\Omega \subseteq \mathbb{C}$  is a connected region with a smooth boundary, and  $T(\xi): \Omega \rightarrow \mathbb{C}^{n \times n}$  is a  $\xi$ -dependent matrix [18, 28]. In the particular case that  $T(\xi)$  is a matrix polynomial in  $\xi$ , (1) is also called a polynomial eigenvalue problem (PEP). Many well-known problems are of this type, such as the Orr–Sommerfeld equation [35] for the incompressible Navier–Stokes equation, and the vibration analysis of the damped beams [20].

Nowadays, an increasing number of non-polynomial NEPs arise from physics, chemistry, and industrial applications. These problems have remarkable practical and theoretical value. But

they are far more complicated to solve due to their large scale and nonlinearity. One emerging example appears in quasi normal mode (QNM) analysis [30], where the computation of a small set of eigentriplets of large, sparse rational eigenvalue problems

$$\sum_{j=1}^p r_j(\lambda) L_j v = 0, \quad r_j(\cdot): \mathbb{C} \rightarrow \mathbb{C}, \quad L_j \in \mathbb{C}^{n \times n}, \quad j = 1, \dots, p$$

is needed for modal expansions, whose results can be used for the physical understanding of nanophotonic devices. Actually, solving rational eigenvalue problems for QNM analysis is currently a very active field; see also [7, 26, 29]. Examples with other nonlinear functions can be found in [21], where nonlinear eigenvalue problems of the form

$$(A + \lambda B + \lambda^2 C)v = e^{i\lambda\tau} S v \quad (2)$$

are to be solved. Here,  $A$ ,  $B$ ,  $C$ , and  $S$  are constant matrices, and  $\tau$  is a scalar. The solution of (2) can be used to obtain the acoustic modes of the Helmholtz wave equation with high efficiency and accuracy.

To address these problems, it may be beneficial to employ Krylov-based methods. This kind of algorithms reformulate the NEP as a generalized eigenvalue problem, and subsequently apply a Krylov algorithm to solve it. Depending on the specific approximations of  $T(\xi)$ , there are Taylor expansion-based algorithms [24], Chebyshev interpolation-based algorithms [25] and, more complicated, rational approximation-based algorithms [8, 19, 38].

Nevertheless, the Krylov-based methods suffer from the drawback that the eigenvalues have to be distributed in certain patterns. For example, Taylor expansion proves unsatisfactory when some eigenvalues are located far away from the expansion point. Chebyshev interpolation, on the other hand, is specifically designed for the eigenvalues lying exactly on the real axis or some pre-specified curves [12]. In some practical applications, users seek for the eigenvalues lying in certain regions, without prior knowledge of their number and distribution. In such cases, to capture all the eigenvalues by a single Taylor expansion point is almost impossible, not to say connecting them with a pre-specified curve. To address this challenge, researchers may employ the rational Krylov method to target multiple points instead of just one. However, there is still no guarantee that all eigenvalues lying in the region of interest can be obtained.

Contour integral-based algorithms are another type of widely-used eigensolvers that are originally developed for linear eigenvalue problems. One of the most representative algorithms, the Sakurai–Sugiura method [32], transforms the original problems into a generalized eigenvalue problem of two small Hankel matrices from which it extracts eigenvalue approximations using standard dense eigensolvers. Nevertheless, computing these eigenvalues can be numerically unstable because the Hankel matrices, formed by higher moments, are usually ill-conditioned. Thus, projection methods such as FEAST [31, 34] and CIRR [33] are developed. Similar to the Sakurai–Sugiura method, these methods approximate the characteristic subspace by integration rules. However, they subsequently apply a projection on this subspace to avoid generating Hankel matrices.

When dealing with non-linear eigenvalue problems, the previously mentioned algorithms have corresponding extensions. In the case of the Sakurai–Sugiura method, all its theories follow and can be directly adapted to NEP cases [2]. However, the same ease does not apply to FEAST or CIRR, because computing an approximate solution of a general NEP on a projection subspace is no longer an easy task. Hence, nonlinear FEAST [16] or CIRR [39] need additionally an auxiliary solver for solving projected problems.

To avoid the numerical instability of the Sakurai–Sugiura method and the uncertainty of nonlinear FEAST and CIRR, we will take Beyn’s algorithm [6] as the eigensolver for this work.

It can be regarded as a nonlinear extension of the Sakurai–Sugiura algorithm using only the first two moments. However, it should be noted that, though Beyn’s algorithm is employed as a framework in this paper, the technique we shall propose is not dependent on a specific eigensolver, but can be extended naturally to any contour integral-based algorithm where several moments need to be computed. A more detailed introduction will be provided later.

Although eigenvalues close to the contour may present certain challenges for contour integral-based algorithms, when compared to Krylov subspace-based algorithms, contour integral-based algorithms are not significantly reliant on the a priori knowledge of the eigenvalue distribution. Hence they are well-suited for extracting all eigenvalues lying in the domain of interest. However, these algorithms require solving a series of linear systems, which could be a heavy workload, especially for large, sparse problems.

Our interest in this work is to solve these linear parameterized systems efficiently. If  $T$  is linear with respect to  $\xi$ , nested Krylov methods, such as multi-shift GMRES [14] or multi-shift QMRIDR [3] can be applied to reuse the Arnoldi basis [1]. Nevertheless, these techniques are designed for linear cases, and cannot be easily extended when the system is not linear with respect to the parameter. In this paper, we employ infinite GMRES [10, 22] to overcome these difficulties. In simple terms, infinite GMRES uses a companion linearization to transform the parameterized system to a form that is linear with respect to the parameter, and then, use multi-shift GMRES to solve multiple systems together.

Briefly, our algorithm solves the NEP using contour integral-based algorithms where the Arnoldi process is employed to solve the linear systems efficiently. It not only avoids the drawback of poor parallelism in Krylov-based algorithms by achieving partial parallelism in matrix factorizations and solving least squares problems, but also significantly reduces the number of LU decompositions required for the contour integral. This makes our algorithm suitable for finding eigenvalues lying within certain contours for large, sparse problems.

The remainder of this paper is organized as follows. In Section 2, we provide a review of Beyn’s algorithm and the infinite GMRES, along with some of their useful properties. In Section 3 we introduce the weighting technique and the two-level orthogonalization technique, and propose the structure of our algorithm. Implementation details, including the selection of some parameters and corresponding analysis, will be discussed in Section 4. Finally, numerical experiments will be presented in Section 5 to illustrate the efficiency of our algorithm.

## 2 Preliminaries

### 2.1 Nonlinear eigenvalue problems

In this work, we focus on nonlinear eigenvalue problems (1), where  $T: \Omega \rightarrow \mathbb{C}^{n \times n}$  is holomorphic in the domain  $\Omega \subset \mathbb{C}$  with sufficiently smooth boundary. Our goal is to find all eigenvalues  $\lambda_1, \dots, \lambda_k$  lying in  $\Omega$ , as well as their corresponding (right) eigenvectors  $v_1, \dots, v_k$ .

We say  $\lambda_j$  is a *simple* eigenvalue if  $\ker(T(\lambda_j)) = \text{span}\{v_j\}$  while  $T'(\lambda_j)v_j \notin \text{Range}(T(\lambda_j))$ . For convenience, in the following, we always assume that there are finitely many eigenvalues lying in  $\Omega$ , and all of them are simple.

### 2.2 Beyn’s algorithm

Beyn’s algorithm [6] can be regarded as a special case of the Sakurai–Sugiura algorithm where only the zeroth moment

$$\mathcal{M}_0 = \frac{1}{2\pi i} \int_{\partial\Omega} T(\xi)^{-1} Z d\xi$$

and first moment

$$\mathcal{M}_1 = \frac{1}{2\pi i} \int_{\partial\Omega} \xi T(\xi)^{-1} Z d\xi$$

are involved. For almost any  $Z \in \mathbb{C}^{n \times k}$ , if we perform the singular value decomposition (SVD),  $\mathcal{M}_0 = V_0 \Sigma_0 W_0^*$ , and construct  $\check{\mathcal{M}}_1 = V_0^* \mathcal{M}_1 W_0 \Sigma_0^{-1}$ , it can be proved that  $\lambda_1, \dots, \lambda_k$  are exactly the eigenvalues of  $\check{\mathcal{M}}_1$ . Furthermore, we can diagonalize  $\check{\mathcal{M}}_1$  as  $\check{\mathcal{M}}_1 = S \Lambda S^{-1}$ , where  $\Lambda = \text{diag}\{\lambda_1, \dots, \lambda_k\}$  so that  $V_0 S = [v_1, \dots, v_k]$  consists of the corresponding eigenvectors of  $T$ .

In Beyn's algorithm, numerical quadrature rules are used to approximate these moments. We assume the boundary of the region,  $\partial\Omega$ , can be parameterized as

$$\varphi \in C^1[0, 2\pi], \quad \varphi(\theta + 2\pi) = \varphi(\theta).$$

Taking  $N$  equidistant quadrature nodes as  $\theta_j = 2j\pi/N$  (for  $j = 0, \dots, N-1$ ) and applying the trapezoidal rule, we will obtain

$$\begin{aligned} \mathcal{M}_{0,N} &= \frac{1}{iN} \sum_{j=0}^{N-1} \varphi'(\theta_j) T(\varphi(\theta_j))^{-1} Z, \\ \mathcal{M}_{1,N} &= \frac{1}{iN} \sum_{j=0}^{N-1} \varphi(\theta_j) \varphi'(\theta_j) T(\varphi(\theta_j))^{-1} Z. \end{aligned} \tag{3}$$

In this work, we always use an ellipse contour

$$\varphi(\theta) = c + a \cos(\theta) + ib \sin(\theta)$$

discretized by the trapezoidal rule with  $N$  equidistant quadrature nodes. This is a usual choice in many works [2, 16, 39], and has been proved to converge exponentially; see [36].

### 2.3 Infinite GMRES

To approximate the moments by (3), we have to evaluate  $T(\xi_j)^{-1} Z$  for several quadrature nodes of the form  $\xi_j = \varphi(\theta_j)$ . With infinite GMRES (infGMRES) [10], we can solve them efficiently.

Suppose we need to compute  $T(\xi)^{-1} z$  for several values of  $\xi$ 's around the origin<sup>1</sup> all at once with infGMRES. We will firstly approximate  $T$  by a Taylor expansion as

$$T(\xi) \approx \sum_{j=0}^p \frac{\xi^j}{j!} T^{(j)}(0),$$

and linearize it to  $\mathcal{L}_0 - \xi \mathcal{L}_1$ , where

$$\mathcal{L}_0 = \begin{bmatrix} T(0) & \frac{T^{(1)}(0)}{1!} & \frac{T^{(2)}(0)}{2!} & \dots & \frac{T^{(p)}(0)}{p!} \\ & I & & & \\ & & I & & \\ & & & \ddots & \\ & & & & I \end{bmatrix}, \quad \mathcal{L}_1 = \begin{bmatrix} 0 & & & & \\ I & 0 & & & \\ & I & \ddots & & \\ & & \ddots & 0 & \\ & & & I & 0 \end{bmatrix}. \tag{4}$$

---

<sup>1</sup>The origin is chosen for simplicity. By a simple change of variable  $\xi \leftarrow \xi - \eta$ , it is easy to perform the computation at arbitrary location on the complex plane.

---

**Algorithm 1** infGMRES
 

---

**Input:** Maximum iteration  $m$ , the parameter-dependent matrix  $T(\xi): \mathbb{C} \rightarrow \mathbb{C}^{n \times n}$ , the right-hand side  $z \in \mathbb{C}^n$  and the points to be solved  $\xi_j$  for  $j = 0, \dots, N-1$

**Output:** Approximations  $x_{0,j} \approx T(\xi_j)^{-1}z$  for  $j = 0, \dots, N-1$

1: Linearize  $T$  to

$$\mathcal{L}_0 = \begin{bmatrix} T(0) & \frac{T^{(1)}(0)}{1!} & \dots & \frac{T^{(p)}(0)}{p!} \\ & I & & \\ & & \ddots & \\ & & & I \end{bmatrix}, \quad \mathcal{L}_1 = \begin{bmatrix} 0 & & & \\ I & 0 & & \\ & \ddots & \ddots & \\ & & I & 0 \end{bmatrix}, \quad p > m$$

2: Perform Arnoldi process on  $(\mathcal{L}_1 \mathcal{L}_0^{-1}, \text{vec}_0(z))$  to obtain  $\mathcal{L}_1 \mathcal{L}_0^{-1} \mathcal{U}_m = \mathcal{U}_{m+1} \underline{H}_m$

3: Set  $y_j \leftarrow \arg \min_y \|(\underline{I}_m - \xi_j \underline{H}_m)y - \|z\|_2 e_1\|_2$  for  $j = 0, \dots, N-1$

4: Set  $x_{0,j} \leftarrow T(0)^{-1} [I \quad -T^{(1)}(0) \quad \dots \quad -T^{(p)}(0)/p!] \mathcal{U}_m y_j$  for  $j = 0, \dots, N-1$

---

It can be proved that the first  $n$  elements of  $(\mathcal{L}_0 - \xi \mathcal{L}_1)^{-1} \text{vec}_0(z)$  are exactly equal to

$$\left( \sum_{j=0}^p \frac{\xi^j}{j!} T^{(j)}(0) \right)^{-1} z, \quad (5)$$

where  $\text{vec}_0(z) = [z^*, 0, \dots, 0]^*$ . Under the assumption that the Taylor expansion is sufficiently accurate, in order to compute  $T(\xi)^{-1}z$ , we just compute  $(\mathcal{L}_0 - \xi \mathcal{L}_1)^{-1} \text{vec}_0(z)$ .

After extracting  $\mathcal{L}_0^{-1}$ , a multi-shift GMRES can be employed to solve for  $(I - \xi \mathcal{L}_1 \mathcal{L}_0^{-1})^{-1} \text{vec}_0(z)$  for several  $\xi$ 's easily. This is because once we obtain

$$\mathcal{L}_1 \mathcal{L}_0^{-1} \mathcal{U}_m = \mathcal{U}_{m+1} \underline{H}_m$$

by the Arnoldi process, we also have

$$(I - \xi \mathcal{L}_1 \mathcal{L}_0^{-1}) \mathcal{U}_m = \mathcal{U}_{m+1} (\underline{I}_m - \xi \underline{H}_m),$$

which is exactly the Arnoldi decomposition of  $I - \xi \mathcal{L}_1 \mathcal{L}_0^{-1}$ . Here,  $\mathcal{U}_m$  is the matrix whose columns are Arnoldi vectors,  $\underline{I}_m$  is the  $m \times m$  identity with an extra zero row at the bottom, and  $\underline{H}_m \in \mathbb{C}^{(m+1) \times m}$  is an upper Hessenberg matrix. Thus, as we already obtained the Hessenberg matrix  $\underline{H}_m$  by an Arnoldi process on  $\mathcal{L}_1 \mathcal{L}_0^{-1}$ , we need only to tackle a small-scale least squares problem

$$y_* = \min_y \|(\underline{I}_m - \xi_* \underline{H}_m)y - \|z\|_2 e_1\|_2, \quad (6)$$

for any certain  $\xi = \xi_*$ . Since  $\mathcal{U}_m y_*$  is the approximate value of  $(I - \xi_* \mathcal{L}_1 \mathcal{L}_0^{-1})^{-1} \text{vec}_0(z)$ , we take  $\mathcal{L}_0^{-1} \mathcal{U}_m y_*$  as the approximate value of  $(\mathcal{L}_0 - \xi_* \mathcal{L}_1)^{-1} \text{vec}_0(z)$ . Then, the first  $n$  elements of  $\mathcal{L}_0^{-1} \mathcal{U}_m y_*$  become the approximate value for  $T^{-1}(\xi_*)z$ . For reference, we list our infGMRES briefly in Algorithm 1. It should be noted that, in the Arnoldi process of Algorithm 1, the matrix-vector multiplications with  $\mathcal{L}_0^{-1}$  and  $\mathcal{L}_1$  can be performed implicitly with matrix-vector multiplications on  $T^{(j)}(0)$ 's and solving linear systems with  $T(0)$ . The matrices  $\mathcal{L}_0$  and  $\mathcal{L}_1$  are never constructed explicitly.

It can be seen that applying  $\mathcal{L}_0^{-1}$  to several vectors involves essentially only one matrix factorization of  $T(0)$ . Hence, infGMRES is efficient when solving with many  $\xi$ 's. Furthermore, in [10],

---

**Algorithm 2** Beyn's method with infGMRES

---

**Input:** The parameter-dependent matrix  $T(\xi): \mathbb{C} \rightarrow \mathbb{C}^{n \times n}$ , the initial guess  $Z = [z_1, \dots, z_k] \in \mathbb{C}^{n \times k}$ , the contour  $\varphi$  and quadrature nodes  $\theta_j$  for  $j = 0, \dots, N-1$

**Output:** Approximate eigenvalues  $\Lambda$  and eigenvectors  $V$

- 1: **for**  $s = 1, \dots, k$  **do**
  - 2:   Use infGMRES to solve for  $T(\varphi(\theta_j))^{-1} z_s$  for  $j = 0, \dots, N-1$  simultaneously
  - 3: **end for**
  - 4: Set  $\mathcal{M}_{0,N} \leftarrow \frac{1}{iN} \sum_{j=0}^{N-1} \varphi'(\theta_j) T(\varphi(\theta_j))^{-1} Z$
  - 5: Set  $\mathcal{M}_{1,N} \leftarrow \frac{1}{iN} \sum_{j=0}^{N-1} \varphi(\theta_j) \varphi'(\theta_j) T(\varphi(\theta_j))^{-1} Z$
  - 6: Singular value decomposition  $\mathcal{M}_{0,N} = V_0 \Sigma_0 W_0^*$
  - 7: Set  $\check{\mathcal{M}}_{1,N} \leftarrow V_0^* \mathcal{M}_{1,N} W_0 \Sigma_0^{-1}$
  - 8: Eigenvalue decomposition  $\check{\mathcal{M}}_{1,N} = S \Lambda S^{-1}$
  - 9: Set  $V \leftarrow V_0 S$
- 

it is proved that under certain mild assumptions the action  $\mathcal{L}_0^{-1}$  can be applied approximately without affecting the convergence of the algorithm. This feature makes infGMRES even more attractive, if implemented properly.

Additionally, we note here that the order of the Taylor expansion,  $p$ , does not need to be determined in advance because at the  $j$ th iteration of GMRES only  $T^{(s)}(0)$ 's with  $s < j$  are involved. If we process up to some certain iterations, say  $j$ , and find that the desired accuracy is not achieved, we can just provide the algorithm with a new  $T^{(j+1)}(0)$  and continue. Therefore, we can always assume that  $p = \infty$ , which means the nonlinear function  $T$  is infinitely approximated by Taylor series within the domain of convergence. That is also why these algorithms are usually called infinite, or hold dynamic polynomial approximation properties [37]. For simplicity, we illustrate the algorithms with the a priori prepared, order  $p > m$ , Taylor expansions in this paper. But readers should keep in mind that the order  $p$  can be increased during the algorithm process and does not need to be decided in advance.

### 3 Proposed algorithm

With the methods we mentioned above, our idea is to solve linear systems in Beyn's method by infGMRES. A framework is summarized in Algorithm 2. In the following paragraphs, we will discuss how to employ infGMRES economically and efficiently in Step 2 of Algorithm 2.

One possible approach is to expand the Taylor series of  $T$  on the center of the contour to approximate all the linear systems on the contour at once. Unfortunately, the original implementation of infGMRES is usually not accurate enough, especially when the ellipse is relatively large or some eigenvalues lie close to the quadrature nodes [10]. To illustrate this, we take the **gun** problem from the NLEVP collection [5] as an example. We apply infGMRES on the center of a circular contour and solve the linear system at each quadrature node; see Figure 1 (left). With 32 GMRES iterations, we obtained completely incorrect solutions.

Though this failure is partly caused by using too few iterations, it is not unavoidable within the same number of iterations. If we instead run infGMRES on the variable-substituted matrix  $T(5a\tilde{\xi} + c)$  to solve the same linear systems, the accuracy can be improved apparently within the same number of iterations; see Figure 1 (right). Here, we take  $a = 45738$  as the radius of the circular contour and  $c = 66762$  as the center of the contour. We first provide a more general framework of this scaling technique in Section 3.1. Detailed analysis will be included in

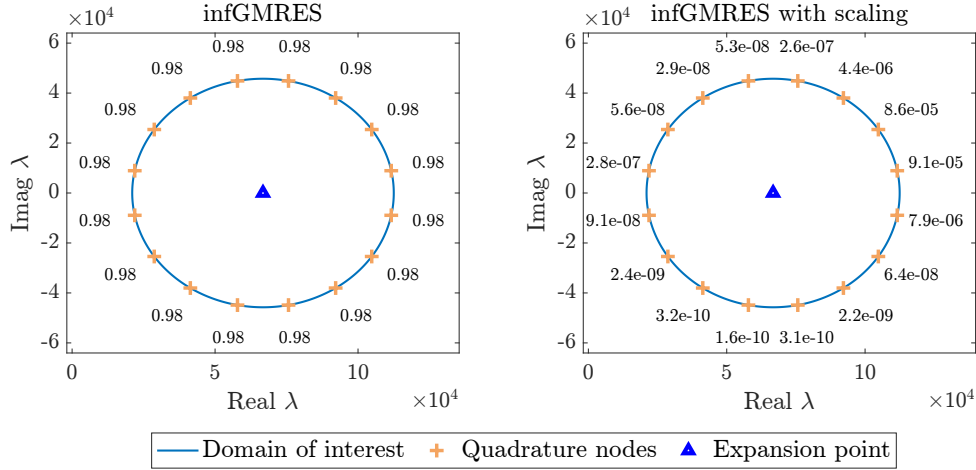


Figure 1: We use infGMRES to solve several linear systems of the `gun` problem. The contour is a circle centered at 66762 with a radius 45738. The quadrature nodes  $\xi_j$  from 16 linear systems,  $T(\xi_j)x = z$ ,  $j = 0, \dots, 15$ , lie equidistantly on the contour. The only Taylor expansion point is located at the center of the contour, and the infGMRES method with  $m = 32$  maximum iterations is used in both figures. To illustrate the accuracy, we plot the relative residuals  $\|T(\xi_j)x_{0,j} - z\|_2 / (\|T(\xi_j)\|_2 \|x_{0,j}\|_2 + \|z\|_2)$ , where  $x_{0,j}$  stands for the approximate solution of the  $j$ th linear system (same terms as in Algorithm 1). In practice, for approximating eigenpairs, we usually need these linear systems to be solved to an accuracy higher than  $10^{-10}$ . The original infGMRES method (left) failed at all 16 points, whereas the infGMRES applied to the variable-substituted system  $T(5a\tilde{\xi} + c)$  (right), although still not accurate enough, demonstrates a seemingly improved performance.

#### Section 4.1.

We remark that, even with the scaling technique, it is impractical to solve the linear systems for all quadrature nodes  $\xi_j$  on the contour with a single Taylor expansion at the center of the contour  $c$ . Actually, it is proved in [22] that the accuracy of the infGMRES decays with the distance to the Taylor expansion point  $|\xi_* - c|$ . Therefore, when employing infGMRES in contour integral-based algorithms, we usually expand the Taylor series at several different points to guarantee that every linear system on the contour can be solved accurately. These points, which are referred to as *the expansion points*, will be discussed in Section 4.3.

The other problem is the redundant memory usage of  $\mathcal{U}_m$ . Storing the whole  $\mathcal{U}_m$ , as classical GMRES does, requires  $\mathcal{O}(m^2n)$  memory. This will greatly limit the maximum iteration count GMRES can take, especially when  $n$  is very large. Following [25], we will apply a TOAR-like technique [27] to compress the memory footprint to  $\mathcal{O}(mn + m^3)$ . We will discuss this technique in more detail in Section 3.2.

### 3.1 Weighting

In [10, Remark 6.2], it has been mentioned that an appropriate scaling can accelerate the convergence of infGMRES. But no proof or theoretical analysis is provided to justify the essential cause. In this subsection, we provide a more general implementation of the scaling. Further insights on this technique and its specific application for accelerating the convergence of infGMRES will be covered in Section 4.1.

When using infGMRES to solve for  $T(\xi_*)^{-1}z$  with a Taylor expansion centered at 0, we are actually solving for

$$(\mathcal{L}_0 - \xi_* \mathcal{L}_1)^{-1} \text{vec}_0(z) = \begin{bmatrix} T_0 & T_1 & \cdots & T_p \\ -\xi_* I & I & & \\ & \ddots & \ddots & \\ & & -\xi_* I & I \end{bmatrix}^{-1} \begin{bmatrix} z \\ 0 \\ \vdots \\ 0 \end{bmatrix},$$

where for simplicity we denote  $T_j = T^{(j)}(0)/j!$ ,  $j = 0, \dots, N-1$ . To apply a scaling here, firstly notice that solving for  $T(\xi)^{-1}z$  at  $\xi = \xi_*$  is equivalent to solving for  $\tilde{T}(\tilde{\xi})^{-1}z$  at  $\tilde{\xi} = \xi_*/\rho$ , where  $\tilde{T}(\tilde{\xi}) = T(\rho\tilde{\xi})$ . Repeating the same linearization process on  $\tilde{T}(\tilde{\xi})$  yields alternative companion matrices of the form

$$\tilde{\mathcal{L}}_0 = \begin{bmatrix} T_0 & \rho T_1 & \rho^2 T_2 & \cdots & \rho^p T_p \\ & I & & & \\ & & I & & \\ & & & \ddots & \\ & & & & I \end{bmatrix}, \quad \tilde{\mathcal{L}}_1 = \mathcal{L}_1. \quad (7)$$

To solve the original system at  $\tilde{\xi} = \xi_*/\rho$ , we solve for

$$\left(\tilde{\mathcal{L}}_0 - \frac{\xi_*}{\rho} \tilde{\mathcal{L}}_1\right)^{-1} \text{vec}_0(z) = \begin{bmatrix} T_0 & \rho T_1 & \cdots & \rho^p T_p \\ -\frac{\xi_*}{\rho} I & I & & \\ & \ddots & \ddots & \\ & & -\frac{\xi_*}{\rho} I & I \end{bmatrix}^{-1} \begin{bmatrix} z \\ 0 \\ \vdots \\ 0 \end{bmatrix}.$$

Comparing (4) and (7), we notice that

$$\tilde{\mathcal{L}}_0 = D_\rho^{-1} \mathcal{L}_0 D_\rho, \quad \frac{1}{\rho} \tilde{\mathcal{L}}_1 = D_\rho^{-1} \mathcal{L}_1 D_\rho, \quad \tilde{\mathcal{L}}_0 - \frac{\xi_*}{\rho} \tilde{\mathcal{L}}_1 = D_\rho^{-1} (\mathcal{L}_0 - \xi_* \mathcal{L}_1) D_\rho,$$

where

$$D_\rho = \begin{bmatrix} I & & & \\ & \rho I & & \\ & & \ddots & \\ & & & \rho^p I \end{bmatrix}.$$

This reminds us the balancing techniques [9] for eigenvalue problems, where we may take

$$D = \begin{bmatrix} d_0 I & & & \\ & d_1 I & & \\ & & \ddots & \\ & & & d_p I \end{bmatrix} \quad (8)$$

with arbitrary  $d_j$ 's. In fact, we can also obtain the approximate solution (5) by solving for  $(D^{-1}(\mathcal{L}_0 - \xi \mathcal{L}_1)D)^{-1} \text{vec}_0(z)$ ; see Lemma 1.



**Lemma 1.** Suppose  $d_j \in \mathbb{C} \setminus \{0\}$  and  $T_j \in \mathbb{C}^{n \times n}$  for  $j = 0, \dots, p$ , and

$$D = \begin{bmatrix} d_0 I & & & & \\ & d_1 I & & & \\ & & \ddots & & \\ & & & d_{p-1} I & \\ & & & & d_p I \end{bmatrix},$$

$$\mathcal{L}_0 = \begin{bmatrix} T_0 & T_1 & T_2 & \cdots & T_p \\ & I & & & \\ & & I & & \\ & & & \ddots & \\ & & & & I \end{bmatrix}, \quad \mathcal{L}_1 = \begin{bmatrix} 0 & & & & \\ I & 0 & & & \\ & I & \ddots & & \\ & & \ddots & 0 & \\ & & & I & 0 \end{bmatrix}.$$

Then, for any scalar  $\xi \in \mathbb{C}$  and vector  $z \in \mathbb{C}^n$ ,

$$(D^{-1}(\mathcal{L}_0 - \xi \mathcal{L}_1)D)^{-1} \text{vec}_0(z) = \begin{bmatrix} (\sum_{j=0}^p \xi^j T_j)^{-1} z \\ * \\ \vdots \\ * \end{bmatrix}.$$

*Proof.* The proof of Lemma 1 follows from [10, Theorem 3.1]. We do not repeat it here.  $\square$

Lemma 1 indicates that we can perform infGMRES on any balanced companion linearization  $(D^{-1}\mathcal{L}_0 D, D^{-1}\mathcal{L}_1 D)$ , and a scaling can be regarded as a special case where  $D = D_\rho$ . Additionally, since  $D^{-1}\mathcal{L}_j D = (d_0^{-1}D)^{-1}\mathcal{L}_j(d_0^{-1}D)$ ,  $j = 0, 1$ , we can always assume  $d_0 = 1$  without loss of generality.

### 3.2 Compact representation of the Arnoldi basis

The two-level orthogonal Arnoldi (TOAR) procedure, initially outlined in [40] (where it is referred to as a compact Arnoldi decomposition), is a memory-efficient algorithm for computing an orthogonal basis of a second-order Krylov subspace, which is widely used for reducing the memory footprint when solving quadratic eigenvalue problems (QEP). The most remarkable insight of TOAR is that the Arnoldi vectors of a companion linearization of the QEP can be represented in terms of a common basis for both upper and lower halves. The TOAR procedure is proved to be numerically stable [27], and a framework is developed to extend this technique to more general cases [38]. In [23], a similar TIAR procedure is implemented on the infinite Arnoldi algorithm from the point of view of a tensor representation. In this work, we extend the idea of two-level orthogonalization to reduce the increasingly larger memory usage.

Firstly, partition the Arnoldi vectors  $\mathcal{U}_m$  by row blocks to

$$\mathcal{U}_m = \begin{bmatrix} U_{m,0} \\ \vdots \\ U_{m,p} \end{bmatrix}, \quad U_{m,j} \in \mathbb{C}^{n \times m}, \quad j = 0, \dots, p.$$

Then, there is a  $Q_m \in \mathbb{C}^{n \times m}$ ,  $Q_m^* Q_m = I$ , such that  $U_{m,j} = Q_m \check{U}_{m,j}$  for some  $\check{U}_{m,j} \in \mathbb{C}^{m \times m}$  (for  $j = 0, \dots, p$ ). Furthermore, the Arnoldi process can be rearranged into

$$\mathcal{L}_1 \mathcal{L}_0^{-1} \mathcal{U}_m = \mathcal{L}_1 \mathcal{L}_0^{-1} \begin{bmatrix} Q_m \check{U}_{m,0} \\ \vdots \\ Q_m \check{U}_{m,p} \end{bmatrix} = \begin{bmatrix} Q_m \check{U}_{m,0} & [Q_m, q_{m+1}] \check{u}_{m+1,0} \\ \vdots & \vdots \\ Q_m \check{U}_{m,p} & [Q_m, q_{m+1}] \check{u}_{m+1,p} \end{bmatrix} \underline{H}_m = \mathcal{U}_{m+1} \underline{H}_m,$$

where  $\underline{H}_m \in \mathbb{C}^{(m+1) \times m}$ ,  $\check{u}_{m+1,j} \in \mathbb{C}^{m+1}$  (for  $j = 0, \dots, p$ ), and the columns of both  $[Q_m, q_{m+1}]$  and

$$\begin{bmatrix} Q_m \check{U}_{m,0} & [Q_m, q_{m+1}] \check{u}_{m+1,0} \\ \vdots & \vdots \\ Q_m \check{U}_{m,p} & [Q_m, q_{m+1}] \check{u}_{m+1,p} \end{bmatrix}$$

are orthonormal. Thus, by setting  $Q_{m+1} = [Q_m, q_{m+1}]$  and

$$\check{U}_{m+1,j} = \left[ \begin{array}{c|c} \check{U}_{m,j} & \check{u}_{m+1,j-1} \\ \hline 0 & \end{array} \right],$$

the Arnoldi vectors  $\mathcal{U}_{m+1}$  share the same structure

$$\mathcal{U}_{m+1} = \begin{bmatrix} Q_{m+1} \check{U}_{m+1,0} \\ \vdots \\ Q_{m+1} \check{U}_{m+1,p} \end{bmatrix}.$$

Therefore, we only need to store  $Q_m$  and  $\check{U}_{m,j}$  in memory for the Arnoldi process. Additionally, thanks to the pattern of  $\text{vec}_0(z)$ , we have  $\check{U}_{m,j} = 0$  for  $j \geq m$ . Overall, the memory usage will be  $\mathcal{O}(mn + m^3)$ . However, since  $\mathcal{U}_m$  is not explicitly formed, additional care should be taken when orthogonalizing, using the so called two-level orthogonalization. Combined with weighting, we list our weighted two-level orthogonal infGMRES in Algorithm 3 for reference.

**Remark 1.** For simplicity and consistency, we initialize  $\check{U}_{j,s}$ 's for  $s = 0, \dots, p$  from the beginning. However, readers should remember that  $\check{U}_{j,s} = 0$  for  $s \geq j$ . Hence,  $\check{U}_{j,s}$ 's are neither computed nor stored in memory.

**Remark 2.** Notice that in Step 4 of Algorithm 1, we have to apply

$$Q_{\log} = T(0)^{-1} \begin{bmatrix} I & -T^{(1)}(0) & \dots & -T^{(p)}(0)/p! \end{bmatrix} \mathcal{U}_m$$

on each  $y_j$  to recover the approximate solution  $x_{0,j}$ , which may involve extra workload. Fortunately, as mentioned in [10], we can store  $Q_{\log}$  column by column during the infGMRES process, to make this cheaper; see Step 6 and Step 19 in Algorithm 3.

**Remark 3.** We remark here that even with the TOAR-like technique,  $Q_m$  and

$$\check{U}_m = \begin{bmatrix} \check{U}_{m,0} \\ \vdots \\ \check{U}_{m,p} \end{bmatrix}$$

may not be fully orthogonal in finite precision arithmetic. As we show in Table 1, Algorithm 3 loses the orthogonality of  $Q_m$  in almost every test example and sometimes loses the orthogonality of  $\check{U}_m$  as well. However, the loss of orthogonality does not always destroy the convergence of GMRES; see [17]. In fact, we can perform a reorthogonalization on  $Q_m$  and  $\check{U}_m$  to make them orthogonal; see Table 1. Nevertheless, the accuracy of infGMRES will not increase, even though both  $Q_m$  and  $\check{U}_m$  are numerically orthogonal. Therefore, we will not use reorthogonalization in our numerical experiments.

---

**Algorithm 3** Weighted two-level orthogonal infGMRES
 

---

**Input:** Maximum iterations  $m$ , the matrices  $T_j \in \mathbb{C}^{n \times n}$  for  $j = 0, \dots, p$ ,  $p > m$ , the initial guess  $z \in \mathbb{C}^n$  and the weights  $d_1, \dots, d_p$

**Output:** A function  $f(\cdot)$  such that  $f(\xi)$  approximates  $T(\xi)^{-1}z$

```

1: function  $[f] = \text{WTinfGMRES}(T_0, \dots, T_p, d_1, \dots, d_p, z)$ 
2:  $Q_1 \leftarrow z/\|z\|_2$ ,  $H_0 \leftarrow [\ ]$ ,  $Q_{\log} \leftarrow [\ ]$ 
3:  $\check{U}_{1,0} \leftarrow 1$ ,  $\check{u}_{1,0} \leftarrow 1$ ,  $\check{U}_{1,s} \leftarrow 0$ ,  $\check{u}_{1,s} \leftarrow 0$ ,  $s = 1, \dots, p$ 
4: for  $j = 1, \dots, m$  do
5:    $q_{j+1} \leftarrow d_1^{-1} T_0^{-1} (Q_j \check{u}_{j,0} - \sum_{s=1}^p d_s T_s Q_j \check{u}_{j,s})$ 
6:    $Q_{\log} \leftarrow [Q_{\log}, d_1 q_{j+1}]$                                      % Record  $\mathcal{L}_0^{-1} Q_j$ 
7:    $l_j \leftarrow Q_j^* q_{j+1}$                                            % First level orthogonalization
8:    $q_{j+1} \leftarrow q_{j+1} - Q_j l_j$ 
9:    $\alpha_j \leftarrow \|q_{j+1}\|_2$ 
10:   $q_{j+1} \leftarrow q_{j+1}/\alpha_j$ 
11:   $Q_{j+1} \leftarrow [Q_j, q_{j+1}]$ 
12:   $h_j = \check{U}_{j,1}^* l_j + \sum_{s=2}^p (d_{s-1}/d_s) \check{U}_{j,s}^* \check{u}_{j,s-1}$            % Second level orthogonalization
13:   $\check{u}_{j+1,0} \leftarrow 0$ ,  $\check{u}_{j+1,1} \leftarrow \begin{bmatrix} l_j - \check{U}_{j,1}^* h_j \\ \alpha_j \end{bmatrix}$ ,  $\check{u}_{j+1,s} \leftarrow \begin{bmatrix} \check{u}_{j,s-1} - \check{U}_{j,s}^* h_j \\ 0 \end{bmatrix}$ ,  $s = 2, \dots, p$ 
14:   $\beta_j \leftarrow \sqrt{\sum_{s=0}^j \check{u}_{j+1,s}^* \check{u}_{j+1,s}}$ 
15:   $\check{u}_{j+1,s} \leftarrow \check{u}_{j+1,s}/\beta_j$ ,  $s = 0, \dots, p$ 
16:   $H_j \leftarrow \begin{bmatrix} H_{j-1} & h_j \\ 0 & \beta_j \end{bmatrix}$                                      % Update  $U$  and  $H$ 
17:   $\check{U}_{j+1,s} \leftarrow \begin{bmatrix} \check{U}_{j,s} & \check{u}_{j+1,s} \\ 0 & \end{bmatrix}$ ,  $s = 0, \dots, p$ 
18: end for
19: return  $f: \xi \mapsto \|z\|_2 Q_{\log} (I - \xi H_m)^\dagger e_1$ 
20: end function

```

---

Table 1: Application of Algorithm 3 with/without reorthogonalization to all 9 test examples from Table 2. The last two columns show the orthogonality of  $Q_m$  and  $\tilde{U}_m$ . The test is performed on all the expansion points, and only the worst values are shown here.

	Problem	$\ Q_m^* Q_m - I\ _2$	$\ \tilde{U}_m^* \tilde{U}_m - I\ _2$
w/o reorthog.	spring	$2.3 \times 10^1$	$6.3 \times 10^{-7}$
	acoustic_wave_2d	$2.1 \times 10^{-8}$	$5.8 \times 10^{-11}$
	butterfly	$7.8 \times 10^{-4}$	$1.4 \times 10^{-3}$
	loaded_string	$1.6 \times 10^1$	$1.5 \times 10^{-13}$
	photonics	$1.9 \times 10^1$	$7.1 \times 10^{-11}$
	railtrack2_rep	$1.7 \times 10^1$	$4.0 \times 10^{-14}$
	hadelar	$1.2 \times 10^{-14}$	$2.0 \times 10^{-14}$
	gun	$1.8 \times 10^1$	$4.0 \times 10^{-14}$
	canyon_particle	$1.9 \times 10^1$	$8.1 \times 10^{-6}$
with reorthog.	spring	$1.1 \times 10^{-15}$	$5.0 \times 10^{-16}$
	acoustic_wave_2d	$6.8 \times 10^{-16}$	$5.0 \times 10^{-16}$
	butterfly	$6.3 \times 10^{-16}$	$6.7 \times 10^{-16}$
	loaded_string	$1.1 \times 10^{-15}$	$7.0 \times 10^{-16}$
	photonics	$7.7 \times 10^{-16}$	$8.1 \times 10^{-16}$
	railtrack2_rep	$5.7 \times 10^{-16}$	$4.3 \times 10^{-16}$
	hadelar	$9.7 \times 10^{-16}$	$3.3 \times 10^{-16}$
	gun	$9.1 \times 10^{-16}$	$7.4 \times 10^{-16}$
	canyon_particle	$9.6 \times 10^{-16}$	$6.7 \times 10^{-16}$

## 4 Implementation details of the algorithm

While our modified infGMRES has been fully described in previous sections, the implementation process involves determining numerous parameters, including the scalars  $d_j$ , the locations of expansion points  $\eta_j$ , and others. In this section, we will reveal the connections among these parameters and the convergence of infGMRES, offering practical guidance on their selection, and hence finishing the last details needed in Algorithm 2.

### 4.1 Scaling is essentially a weighting strategy on GMRES

In Section 3.1, we have already showed that a scaling can be generalized into a balanced companion linearization, say  $D^{-1}\mathcal{L}_0 D$  and  $D^{-1}\mathcal{L}_1 D$ . Here, we declare that this technique is essentially a weighting strategy for the least squares problems within GMRES, which is very similar to the weighted GMRES algorithm [13]. If used appropriately, this technique can help to find a more accurate solution in a certain search space.

To see this, we have to look into the process of GMRES. First notice that if the Krylov subspace  $\mathcal{K}_m(I - \xi_* \mathcal{L}_1 \mathcal{L}_0^{-1}, \text{vec}_0(z))$  is spanned by  $\mathcal{U}_m$ , by induction, we can prove that  $\mathcal{K}_m(D^{-1}(I - \xi_* \mathcal{L}_1 \mathcal{L}_0^{-1})D, \text{vec}_0(z))$  is spanned by  $D^{-1}\mathcal{U}_m$ . Thus, at the  $m$ th iteration, infGMRES will give the solution by

$$\begin{aligned}
y_* &= \arg \min_y \|D^{-1}(I - \xi_* \mathcal{L}_1 \mathcal{L}_0^{-1})DD^{-1}\mathcal{U}_m y - \text{vec}_0(z)\|_2 \\
&= \arg \min_y \|D^{-1}((I - \xi_* \mathcal{L}_1 \mathcal{L}_0^{-1})\mathcal{U}_m y - \text{vec}_0(z))\|_2,
\end{aligned} \tag{9}$$

where the last equality follows because  $d_0 = 1$ .

Equation (9) provides us with several insights. Firstly, irrespective of the selection of the weighting matrix  $D$ , the final approximation of  $T(\xi_*)^{-1}z$  will be selected from the same search space. That is because the approximate solution will be the first  $n$  elements of  $D^{-1}\mathcal{L}_0^{-1}\mathcal{U}_m y_*$  and  $d_0 = 1$ . The role  $D$  plays in infGMRES is actually a weighting matrix in the least squares problems (9). We can choose  $D$  appropriately to guide GMRES to pick a more accurate solution from  $\mathcal{U}_m$ .

The previous sentence may seem contradictory because GMRES already provides the best solution that minimizes the residual norm. However, what we really care about is not the residual of GMRES (9), but

$$\|r_N\|_2 = \|T(\xi_*)x_{0,*} - z\|_2,$$

where  $x_{0,*}$  is the approximate value of  $T(\xi_*)^{-1}z$ . Since

$$\|r_N - r_P\|_2 = \left\| \frac{T^{(p+1)}(\zeta)}{(p+1)!} \xi_*^{n+1} \right\|_2 \leq \frac{\|T^{(p+1)}(\zeta)\|_2}{(p+1)!} \|\xi_*\|_2^{n+1}, \quad \zeta = \delta \xi_*, \quad \delta \in (0, 1),$$

we can instead consider

$$\|r_P\|_2 = \left\| \sum_{j=0}^p \xi_*^j T_j x_{0,*} - z \right\|_2 \quad (10)$$

when  $\mathcal{O}(\|T^{(p+1)}(\zeta)\|_2 \|\xi_*\|_2^{n+1} / (p+1)!)$  is negligible. In an ideal scenario, we choose the weighting matrix  $D$  so that (9) returns the best solution in the sense of (10). Therefore, it is crucial to reveal the relationship between (9) and (10).

**Lemma 2.** Suppose  $z$ ,  $\mathcal{U}_m$ ,  $\mathcal{L}_0$ ,  $\mathcal{L}_1$  and  $T_j$  (for  $j = 0, \dots, p$ ) are all defined as before. The vector  $y_* \in \mathbb{C}^m$  is the solution of (9) for some weighting matrix  $D$ . Then, the polynomial-wise residual  $r_P = \sum_{j=0}^p \xi_*^j T_j x_{0,*} - z$  can be represented as

$$r_P = \left[ I, -\sum_{j=1}^p \xi_*^{j-1} T_j, -\sum_{j=2}^p \xi_*^{j-2} T_j, \dots, -T_p \right] \begin{bmatrix} r_0 \\ r_1 \\ \vdots \\ r_p \end{bmatrix}, \quad (11)$$

where

$$\begin{bmatrix} r_0 \\ r_1 \\ \vdots \\ r_p \end{bmatrix} = (I - \xi_* \mathcal{L}_1 \mathcal{L}_0^{-1}) \mathcal{U}_m y_* - \text{vec}_0(z). \quad (12)$$

*Proof.* We know that if  $y_*$  is the solution of (9), infGMRES will give  $x_* = D^{-1}\mathcal{L}_0^{-1}\mathcal{U}_m y_*$  as the approximate value of  $(D^{-1}(\mathcal{L}_0 - \xi_* \mathcal{L}_1)D)^{-1} \text{vec}_0(z)$ . Then, by Lemma 1, the first  $n$  elements of  $x_*$ , denoted by  $x_{0,*} \in \mathbb{C}^n$ , will be taken as the approximate value of  $T(\xi_*)^{-1}z$ . In other words, we have

$$D^{-1}\mathcal{L}_0^{-1}\mathcal{U}_m y_* = x_* = \begin{bmatrix} x_{0,*} \\ x_{1,*} \\ \vdots \\ x_{p,*} \end{bmatrix},$$

where  $x_{0,*}$  here is same as the one in (10).

Therefore, we can represent (12) in terms of  $x_*$  instead of  $y_*$ :

$$\begin{bmatrix} r_0 \\ r_1 \\ \vdots \\ r_p \end{bmatrix} = (I - \xi_* \mathcal{L}_1 \mathcal{L}_0^{-1}) \mathcal{U}_m y_* - \text{vec}_0(z) = (\mathcal{L}_0 - \xi_* \mathcal{L}_1) D x_* - \text{vec}_0(z). \quad (13)$$

Just listing out the equations in (13)

$$\begin{aligned} d_0 T_0 x_{0,*} + d_1 T_1 x_{1,*} + \cdots + d_p T_p x_{p,*} &= r_0 + z, \\ -\xi_* d_0 x_{0,*} + d_1 x_{1,*} &= r_1, \\ &\vdots \\ -\xi_* d_{p-1} x_{p-1,*} + d_p x_{p,*} &= r_p, \end{aligned}$$

and substituting all other equations into the first one yields (11).  $\square$

Remember that the solution  $y_*$  minimizes (9), so that  $r_j$ 's minimize

$$\|D^{-1}((I - \xi_* \mathcal{L}_1 \mathcal{L}_0^{-1}) \mathcal{U}_m y_* - \text{vec}_0(z))\|_2 = \left\| D^{-1} \begin{bmatrix} r_0 \\ r_1 \\ \vdots \\ r_p \end{bmatrix} \right\|_2 = \sqrt{\sum_{j=0}^p \frac{\|r_j\|_2^2}{d_j^2}},$$

which means we can adjust the magnitude of  $r_j$  by setting  $d_j$  properly. If we set  $d_j$  to be larger, then,  $\|r_j\|_2$  must be more modest.

On the other hand, we know from Lemma 2 that

$$\|r_P\|_2 \leq \|r_0\|_2 + \left\| \sum_{j=1}^p \xi_*^{j-1} T_j \right\|_2 \|r_1\|_2 + \cdots + \|T_p\|_2 \|r_p\|_2.$$

Therefore, intuitively, if we make  $\|r_j\|_2$  relatively small for larger  $\|\sum_{j=s}^p \xi_*^{j-s} T_j\|_2$ , and relatively large for smaller  $\|\sum_{j=s}^p \xi_*^{j-s} T_j\|_2$ , overall,  $\|r_P\|_2$  could be modest.

With this insight, we may set the weights as  $d_0 = 1$  and  $d_s = \|\sum_{j=s}^p \xi_*^{j-s} T_j\|_2^{-1}$  for  $s = 1, \dots, p$ . However, there are cases where  $\|\sum_{j=s}^p \xi_*^{j-s} T_j\|_2 \ll 1$  or  $\|\sum_{j=s}^p \xi_*^{j-s} T_j\|_2 \gg 1$ , which will make  $D$  extremely ill-conditioned. Thus, in practice, we prefer to balance  $d_j$  by

$$d_j \leftarrow d_j \cdot \frac{d_2}{d_1^2}, \quad j > 0.$$

Consequently, for a certain quadrature node  $\xi_*$ , a reasonable choice of weights  $d_j$  is:

$$d_0 = 1, \quad d_s = \frac{\gamma}{\|\sum_{j=s}^p \xi_*^{j-s} T_j\|_2}, \quad \gamma = \frac{\|\sum_{j=1}^p \xi_*^{j-2} T_j\|_2^2}{\|\sum_{j=2}^p \xi_*^{j-3} T_j\|_2}, \quad s = 1, \dots, p.$$

**Remark 4** (How to determine  $d_j$ 's in practice). *It is impractical to assign a different weighting matrix  $D$  to each quadrature node, since a different  $D$  results in a different Arnoldi process, which is very expensive and contradicts our original intention. A wiser strategy is to use the*

same  $D$  for all the quadrature nodes under a given expansion point  $\eta_t$ . In practice, we set the weights as

$$d_0 = 1, \quad d_s = \frac{\gamma}{\|\sum_{j=s}^p \nu^{j-s} T_j\|_2}, \quad \gamma = \frac{\|\sum_{j=1}^p \nu^{j-2} T_j\|_2^2}{\|\sum_{j=2}^p \nu^{j-3} T_j\|_2}, \quad s = 1, \dots, p, \quad (14)$$

where

$$\nu = 2 \cdot \max_{j \in \Psi} |\xi_j - \eta_t|, \quad \Psi = \{j : |\xi_j - \eta_t| < |\xi_j - \eta_s|, \ s \neq t\}.$$

This choice performs well in numerical experiments.

**Remark 5.** Our analysis does not depend on specific styles of the companion linearizations. For example, if we use the classical companion linearization

$$\mathcal{L}_0 = \begin{bmatrix} A_1 & A_2 & \cdots & A_p \\ I & & & \\ & \ddots & & \\ & & I & \end{bmatrix}, \quad \mathcal{L}_1 = \begin{bmatrix} A_0 & & & \\ & -I & & \\ & & \ddots & \\ & & & -I \end{bmatrix},$$

it can also be proved that

$$D_\rho^{-1}(\xi \mathcal{L}_1^{-1} \mathcal{L}_0 - I) D_\rho = \frac{\xi}{\rho} \tilde{\mathcal{L}}_1^{-1} \tilde{\mathcal{L}}_0 - I,$$

where  $\tilde{\mathcal{L}}_0$  and  $\tilde{\mathcal{L}}_1$  are the companion linearization matrices corresponding to the scaled system  $\tilde{T}$ . Other analyses on  $D$  will follow.

## 4.2 On polynomial eigenvalue problems

Since infGMRES is originally designed for non-polynomial eigenvalue problems, additional care must be taken when dealing with a PEP, or in other words when

$$T(\xi) = T_0 + \xi T_1 + \cdots + \xi^g T_g.$$

In these cases, it is not necessary for us to use infGMRES. On the contrary, just linearizing it to

$$\check{\mathcal{L}}_0 = \begin{bmatrix} T_0 & T_1 & T_2 & \cdots & T_g \\ & I & & & \\ & & I & & \\ & & & \ddots & \\ & & & & I \end{bmatrix}, \quad \check{\mathcal{L}}_1 = \begin{bmatrix} 0 & & & & \\ I & 0 & & & \\ & I & \ddots & & \\ & & \ddots & 0 & \\ & & & I & 0 \end{bmatrix}, \quad (15)$$

and using multi-shift GMRES to solve for  $(\check{\mathcal{L}}_0 - \xi \check{\mathcal{L}}_1)^{-1} \text{vec}_0(z)$  is sufficient to solve the problem.

However, if infGMRES is chosen, the linearization becomes

$$\mathcal{L}_0 = \begin{bmatrix} T_0 & T_1 & \cdots & T_g & 0 & \cdots \\ & I & & & & \\ & & \ddots & & & \\ & & & I & & \\ & & & & I & \\ & & & & & \ddots \end{bmatrix}, \quad \mathcal{L}_1 = \begin{bmatrix} 0 & & & & & \\ I & 0 & & & & \\ & I & \ddots & & & \\ & & \ddots & 0 & & \\ & & & I & 0 & \\ & & & & \ddots & \ddots \end{bmatrix}, \quad (16)$$

where we use 0 to fill the position of  $T_j$ ,  $j > g$  because  $T^{(j)}(\xi) = 0$ ,  $j > g$ . It is interesting to note that  $(\mathcal{L}_0 - \xi \mathcal{L}_1)^{-1} \text{vec}_0(z)$  also gives the true value of  $T(\xi)^{-1}z$  on the first  $n$  elements. A question naturally arises — is there any performance difference between (15) and (16)?

From the point of view of computational cost and memory usage, in the  $j$ th iteration of (15), the cost of orthogonalization will be  $\mathcal{O}(jn + j^2g)$  and the total memory usage is also  $\mathcal{O}(jn + j^2g)$ . As for (16), they are  $\mathcal{O}(jn + j^3)$ . For general cases  $m > g$ , so that (15) is cheaper. However, since  $g < m \ll n$ , there is not much difference.

Things become interesting if we look from the perspective of convergence rate. Equation (15) can actually be regarded as (16) with the weighting we mentioned in Section 4.1. Remember that, with our weighting strategy, the weighting matrix  $D$  will be

$$D = \begin{bmatrix} d_0 I & & & & & \\ & d_1 I & & & & \\ & & \ddots & & & \\ & & & d_g I & & \\ & & & & \infty I & \\ & & & & & \ddots \end{bmatrix}.$$

Then, if we regard  $\infty$  as a very large number that can be used in arithmetic computation, we will have the weighted system

$$D^{-1} \mathcal{L}_0 D = \begin{bmatrix} T_0 & T_1 & \cdots & T_g & 0 & \cdots \\ & I & & & & \\ & & \ddots & & & \\ & & & I & & \\ & & & & I & \\ & & & & & \ddots \end{bmatrix},$$

$$D^{-1} \mathcal{L}_1 D = \begin{bmatrix} 0 & & & & & \\ \frac{d_0}{d_1} I & 0 & & & & \\ & \ddots & \ddots & & & \\ & & \ddots & \ddots & & \\ & & & \frac{d_{g-1}}{d_g} I & 0 & \\ & & & & 0 & 0 \\ & & & & & I & 0 \\ & & & & & & \ddots & \ddots \end{bmatrix}.$$

Notice that  $D^{-1} \mathcal{L}_1 \mathcal{L}_0^{-1} D$  is a diagonal block matrix now. Since the right-hand side  $\text{vec}_0(z)$  has non-zero elements only on the first  $n$  dimensions, solving for  $(D^{-1}(I - \xi \mathcal{L}_1 \mathcal{L}_0^{-1})D)^{-1} \text{vec}_0(z)$  and  $(D_g^{-1}(I - \xi \check{\mathcal{L}}_1 \check{\mathcal{L}}_0^{-1})D_g)^{-1} \text{vec}_0(z)$  with GMRES will result in exactly the same process, where  $D_g = \text{diag}\{d_0 I, \dots, d_g I\}$  is the truncated  $D$ .

Since both the cost and the convergence of the two methods are similar, we also use infGMRES in Section 5 for PEP to keep results uniform.

### 4.3 Selecting multiple expansion points

Even with the weighting strategy, it may still take too many iterations for infGMRES to converge, especially for quadrature nodes that are far from expansion points. Therefore, it is sensible to



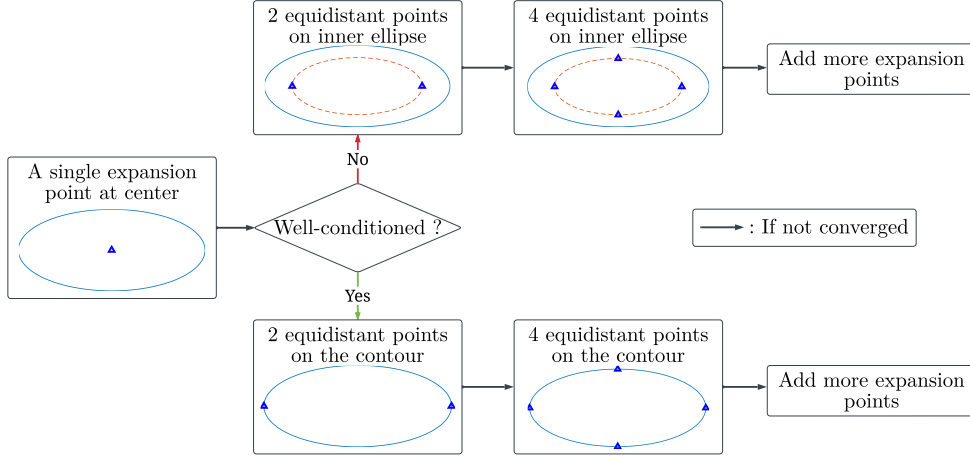


Figure 2: A brief guideline on choosing expansion points: If a single point at the center does not work, choose expansion points equidistantly on the contour or on an inner ellipse, based on the condition number of the problem. Continue doubling the number of expansion points till the accuracy is satisfactory.

use more than one expansion point in practice. However, a good choice of the expansion points depends on the singularities, eigenvalues and many other things. Therefore, adaptively selecting the expansion points is usually impractical, and it is not the focus of interest in this paper. In this subsection, we provide a flowchart for users to heuristically determine the distribution of expansion points; see Figure 2.

At this point, we can fully describe the computation needed for Step 2 of Algorithm 2; see Algorithm 4.

---

**Algorithm 4** Step 2 of Algorithm 2

---

**Input:** The parameter-dependent matrix  $T(\xi): \mathbb{C} \rightarrow \mathbb{C}^{n \times n}$ , the right-hand side  $z \in \mathbb{C}^n$ , the contour  $\varphi$  and quadrature nodes  $\theta_j$  for  $j = 0, \dots, N-1$

**Output:** Approximations  $x_{0,j} \approx T(\varphi(\theta_j))^{-1} z$  for  $j = 0, \dots, N-1$

- 1: Determine expansion points  $\eta_0, \dots, \eta_{n_{ep}}$  as in Figure 2
  - 2: **for**  $j = 0, \dots, n_{ep}$  **do**
  - 3:   Set  $T_{s,j} \leftarrow T^{(s)}(\eta_j)/s!$  for  $s = 0, \dots, p$
  - 4:   Compute weights  $d_{s,j}$  as in Section 3.1
  - 5:   Set  $f_j(\cdot) \leftarrow \text{WTinfGMRES}(T_{0,j}, \dots, T_{p,j}, d_{0,j}, \dots, d_{p,j}, z)$  (Algorithm 3)
  - 6: **end for**
  - 7: **for**  $j = 0, \dots, N-1$  **do**
  - 8:   Find  $\eta_s \in \{\eta_0, \dots, \eta_{n_{ep}}\}$  closest to  $\varphi(\theta_j)$
  - 9:   Set  $x_{0,j} \leftarrow f_s(\varphi(\theta_j))$
  - 10: **end for**
- 

**Remark 6** (Accuracy of linear systems and the quadrature rule). *In contour integral-based algorithms, the number of quadrature nodes is sometimes increased in order to improve the accuracy of the quadrature rule. The question thus arises as to whether the accuracy of the solution of linear*

systems should also be increased. Furthermore, in order to attain a specific level of accuracy for the quadrature rule, how accurate should the linear systems be solved? To the best of our knowledge, this is still an open problem. Nevertheless, in this work, we recommend the users always solve the linear systems to machine precision. This is because of the fact that adding quadrature nodes introduces little additional overhead in our algorithm. Therefore, a well-distributed expansion point set can be reused whenever the users need a higher level of accuracy.

**Remark 7** (Balancing between iterations of infGMRES and number of expansion points). *Having already addressed the question of the desired level of accuracy for linear systems, it is now necessary to consider how this accuracy can be achieved. Two principal parameters can be adjusted — the iterations of infGMRES and the number of expansion points. In practice, it can be observed that increasing the iterations of infGMRES sometimes only leads to slight improvements on the accuracy of solutions of the linear systems. There are several potential explanations for this, including the fact that the convergence radius of the Taylor expansion is limited, or that the convergence of infGMRES is affected by the eigenvalues around. However, increasing the iterations quadratically increases the cost of the orthogonalization of the Arnoldi process and the cost of solving Hessenberg systems, making the algorithm extremely slow. Thus, it is too expensive to request highly accurate solutions by performing many iterations of infGMRES — a wiser choice is to fix the infGMRES iterations and increase the number of expansion points.*

## 5 Numerical experiments

In this section we present experimental results of Algorithms 3. All numerical experiments were performed using MATLAB R2022b on a Linux server with two 16-core Intel Xeon Gold 6226R 2.90 GHz CPUs and 1024 GB main memory.

### 5.1 Experiment settings

Most of our test examples are chosen from the NLEVP collections [5] except **photonics**, which is similar to the one described in [11], but with a more general model for the permittivity as in [15]. We set the maximum number of the outer iterations of infGMRES as 32 for all these examples, while the number of quadrature nodes and expansion points varies from case to case. Details regarding these examples, including their respective types, the problem size  $n$ , the number of quadrature nodes  $N$ , and the number of expansion points  $n_{\text{ep}}$ , are listed in Table 2. For the exact distribution of these points or the contour, readers can check Figure 3.

For computed approximate nonlinear eigenpair  $(\hat{\lambda}, \hat{v})$ , the convergence criterion is

$$\|T(\hat{\lambda})\hat{v}\|_2 \leq \text{tol} \cdot \|T(\hat{\lambda})\|_2 \|\hat{v}\|_2, \quad (17)$$

where  $\text{tol}$  is the user-specified tolerance. Unless otherwise stated, all the test results presented in this section achieved an accuracy of  $\text{tol} = 10^{-12}$ .

As we mentioned in Section 2.3, it is possible to apply the action  $T_0^{-1}$  in Algorithm 3 in an inexact way, e.g., using algebraic multigrid or GMRES, to make the algorithm even faster. However, to emphasize the effect of our algorithm, we use LU decomposition to solve all the linear systems exactly in our numerical experiments. Readers should keep in mind that, in practice, inexact linear solvers can be implemented here for further acceleration.

### 5.2 Overall performance on the test examples

To illustrate the efficiency of our algorithm, we solve the linear systems by MATLAB backslash (`\`) as comparative experiments. The times consumed by Beyn’s method with MATLAB backslash

Table 2: Information of test problems. Here,  $n$  is the size of the problem and  $k$  is the number of the eigenvalues to be computed. The number of quadrature nodes, expansion points are represented by  $N$  and  $n_{\text{ep}}$ , respectively. The times consumed by Beyn’s method with MATLAB backslash,  $t_s$ , and with infGMRES  $t_{\text{iG}}$  are also listed in the last columns.

Problem	Type	$n$	$k$	$N$	$n_{\text{ep}}$	$t_s(\text{s})$	$t_{\text{iG}}(\text{s})$	$(t_s - t_{\text{iG}})/t_s$
spring	QEP	3000	32	1024	6	3.472	15.72	−353%
acoustic_wave_2d	QEP	9900	10	512	5	28.14	9.475	66%
butterfly	PEP	5000	9	512	9	11.54	8.453	27%
loaded_string	REP	20000	10	128	4	1.07	9.805	−816%
photonics	REP	20363	16	3060	18	600	209.7	65%
railtrack2_rep	REP	35955	2	128	1	533.4	71.95	87%
hadeler	NEP	5000	13	32	1	40.2	46.6	−16%
gun	NEP	9956	21	1024	10	501.2	148.9	70%
canyon_particle	NEP	16281	5	256	4	40.94	7.652	81%

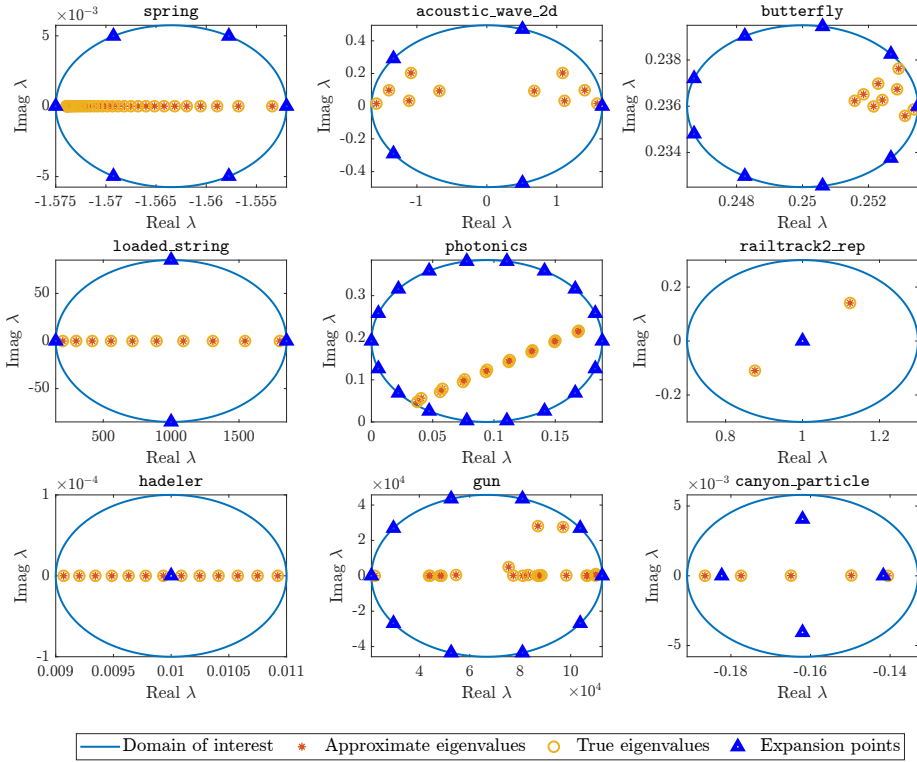


Figure 3: Interest field, expansion points and eigenvalues of different test problems.

$(t_s)$  and with infGMRES ( $t_{\text{iG}}$ ) are listed, respectively, in the last columns of Table 2. Except for the **spring**, **loaded\_string** and **hadeler**, our algorithm achieved a speedup of at least 27%. The acceleration rate increases when the problems size becomes larger, where our algorithm can benefit from taking fewer matrix decompositions and reach a speedup over 80%.

However, there are two scenarios where the advantages of our algorithm are less evident. In the cases of **spring** and **loaded\_string**, MATLAB implements specialized optimizations

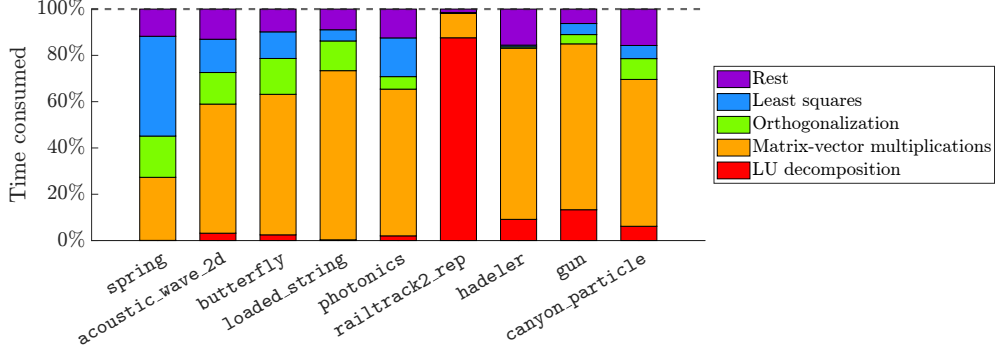


Figure 4: The proportional chart of Beyn’s methods with infinite GMRES. The times consumed by different operations are illustrated.

for tridiagonal matrices, making it several times faster than the general MATLAB backslash operation. On the other hand, in the case of `hadeler`, two out of its three component matrices are dense. Generally, iterative methods are not as efficient for dense matrices, leading to reduced effectiveness in these specific instances.

To obtain a more detailed analysis, we have extracted the time proportions of each operation, as illustrated in Figure 4. It can be found that a significant portion of time is dedicated to the Arnoldi process (matrix–vector multiplications and orthogonalization) in our algorithm. Even in the challenging problem `photonics`, where over 3000 quadrature nodes are needed to be solved, solving least squares problems consume comparatively less time. This implies that our algorithm proves especially advantageous in cases involving a large number of quadrature nodes.

One thing to note from Figure 4 is that the time consumed by LU decomposition is relatively higher for `railtrack2_rep`. That is because the size of this problem is obviously larger, bringing about more expensive factorizations. However, it is actually a good news for our algorithm, which means that when the problem size becomes larger, our algorithm can benefit more from solving these factorizations in parallel.

### 5.3 Comparison on different weighting strategies

In Section 3.1, we introduce a weighting strategy for infGMRES. Here, we illustrate its efficiency under different circumstances with numerical experiments. The `gun` problem is taken as the test problem. We compute the Taylor expansion on the leftmost and rightmost points of the contour, respectively, to approximate the linear systems corresponding to quadrature nodes around. The difference between these two points is that there are singularities close to the left side one, leading to a more ill-conditioned problem. The full picture can be found in Figure 5 (a), where we illustrate the corresponding relationships between expansion points and quadrature nodes. The number of outer iterations of infGMRES is fixed to 32 in all experiments. The residuals obtained with or without weighting can be found in Figures 5 (b), (c), (f), (g). Our weighting strategy can bring significant boost on the accuracy in both cases.

As a comparison, we refer to the scaling strategy from [4, Section 6]. In that algorithm, a scalar

$$\rho = \left( \frac{\|T_0\|_2}{\|T_p\|_2} \right)^{1/p} \quad (18)$$

is used to make the norm of  $\rho^j T_j$  as similar as possible. Their consideration is that solving a

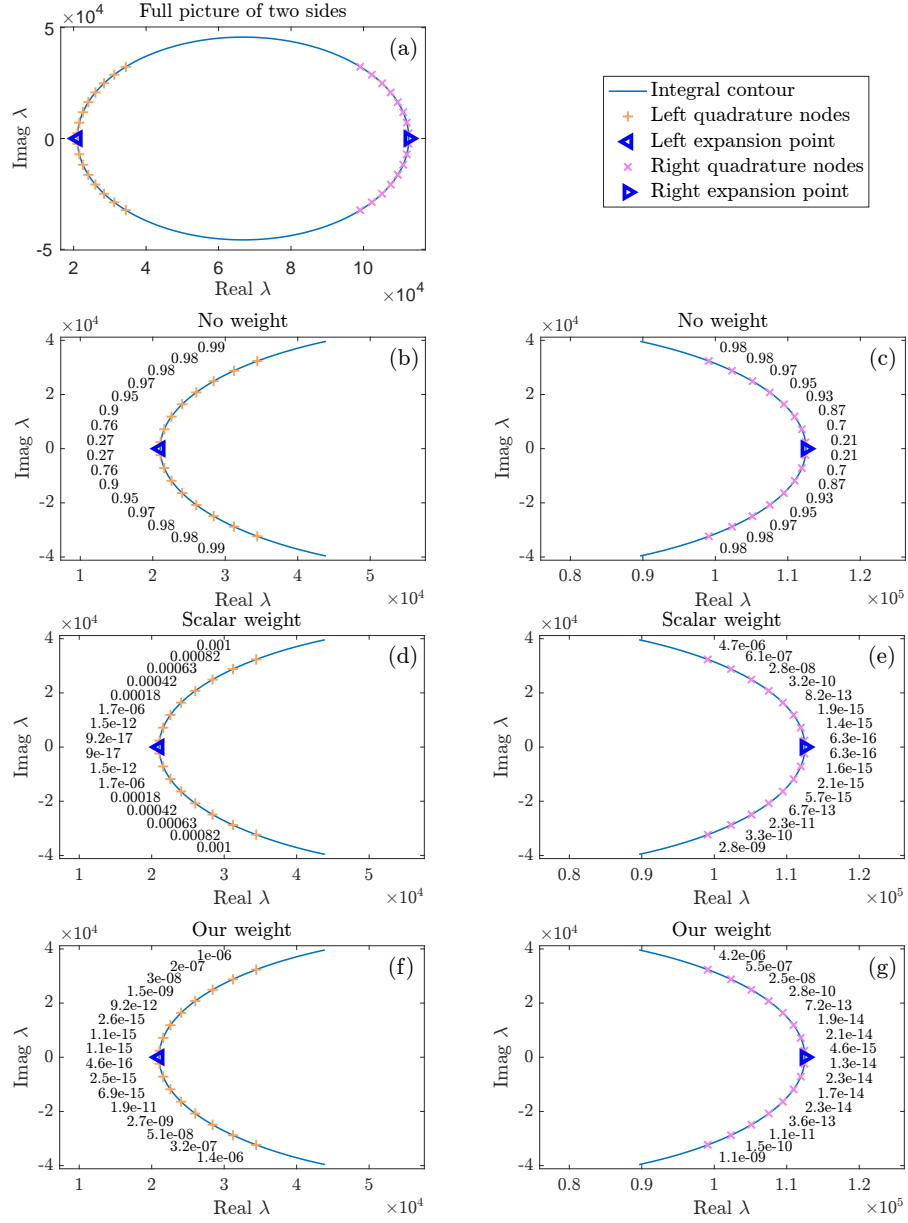


Figure 5: Solving linear systems of the **gun** problem by infGMRES without weighting (b, c), with scaling weighting (18) (d, e) and with our weighting (14) (f, g). (a) shows a full picture of the distribution of the expansion points and part of the quadrature nodes. The residuals plotted in the figures are the relative residuals of solving linear systems. For a certain quadrature node  $\xi_j$ , the relative residual is defined as  $\|T(\xi_j)x_{0,j} - z\|_2 / (\|T(\xi_j)\|_2 \|x_{0,j}\|_2 + \|z\|_2)$ , where  $x_{0,j}$  stands for the approximate solution.

PEP by applying a backward stable algorithm is backward stable if

$$\|T_0\|_2 = \|T_1\|_2 = \cdots = \|T_p\|_2.$$

Even though this algorithm is designed for eigenvalue problems but not for solving linear systems, it shares similar motivations with our algorithm. We implement it in Figure 5 (d), (e). It can be found that, both strategies perform well for well-conditioned cases. Nevertheless, the accuracy of (18) decays rapidly in the ill-conditioned case; see Figure 5 (d); while our algorithm performs obviously better; see Figure 5 (f).

## 6 Conclusion

In this work, we introduce infGMRES to reduce the cost of solving linear systems in contour integral-based nonlinear eigensolvers. We have worked out implementation details including the convergence-accelerating weighting strategy, the memory-friendly TOAR-like trick, and the selection of the parameters. With these ingredients, we proposed a robust and efficient implementation of infGMRES. While our numerical experiments are carried out in Beyn’s method, this technique can actually be applied to all contour integral-based nonlinear eigensolvers, where several moments are needed to be approximated.

Our method reduces the computational cost by reducing the number of required matrix factorizations. More precisely, it requires as many factorizations as the number of expansion points, which is usually much smaller than the number of quadrature nodes. This is especially relevant for difficult problems, where the quadrature rule demands a large number of quadrature nodes or the scale is extremely large, making a matrix decomposition very expensive.

Our future work may involve developing a machine learning-based adaptive strategy for selecting expansion points automatically. Additionally, we may implement a block variant of infGMRES to efficiently solve all right-hand sides.

## Acknowledgments

We would like to thank Guillaume Demésy for providing us with the data from the photonics test case. Furthermore, we would like to express our gratitude to the anonymous reviewers. Their feedback has been instrumental in enhancing this work.

Y. Liu and M. Shao were partly supported by the National Natural Science Foundation of China under grant No. 92370105. J. E. Roman was supported by grant PID2022-139568NB-I00 funded by MICIU/AEI/10.13039/501100011033 and by ERDF/EU, and by grant RED2022-134176-T. This work was carried out while Y. Liu was visiting Universitat Politècnica de València.

## References

- [1] Junko Asakura, Hiroto Sakurai, Tetsuya Tadano, Tsutomu Ikegami, and Kinji Kimura. A numerical method for polynomial eigenvalue problems using contour integral. *Japan J. Indust. Appl. Math.*, 27(1):73–90, 2010. doi:10.1007/s13160-010-0005-x.
- [2] Junko Asakura, Tetsuya Sakurai, Hiroto Tadano, Tsutomu Ikegami, and Kinji Kimura. A numerical method for nonlinear eigenvalue problems using contour integrals. *JSIAM Lett.*, 1:52–55, 2009. doi:10.14495/jsiaml.1.52.
- [3] Manuel Baumann and Martin B. Van Gijzen. Nested Krylov methods for shifted linear systems. *SIAM J. Sci. Comput.*, 37(5):S90–S112, 2015. doi:10.1137/140979927.
- [4] Timo Betcke. Optimal scaling of generalized and polynomial eigenvalue problems. *SIAM J. Matrix Anal. Appl.*, 30(4):1320–1338, 2009. doi:10.1137/070704769.

- [5] Timo Betcke, Nicholas J. Higham, Volker Mehrmann, Christian Schröder, and Françoise Tisseur. NLEVP: A collection of nonlinear eigenvalue problems. *ACM Trans. Math. Software*, 39(2):1–28, 2013. doi:10.1145/2427023.2427024.
- [6] Wolf-Jürgen Beyn. An integral method for solving nonlinear eigenvalue problems. *Linear Algebra Appl.*, 436(10):3839–3863, 2012. doi:10.1016/j.laa.2011.03.030.
- [7] Felix Binkowski, Fridtjof Betz, Rémi Colom, Patrice Genevet, and Sven Burger. Poles and zeros in non-Hermitian systems: Application to photonics. *Phys. Rev. B*, 109(4):045414, 2024. doi:10.1103/PhysRevB.109.045414.
- [8] Carmen Campos and Jose E. Roman. NEP: a module for the parallel solution of nonlinear eigenvalue problems in SLEPc. *ACM Trans. Math. Software*, 47(3):1–29, 2021. doi:10.1145/3447544.
- [9] Tzu-Yi Chen and James W. Demmel. Balancing sparse matrices for computing eigenvalues. *Linear Algebra Appl.*, 309(1-3):261–287, 2000. doi:10.1016/S0024-3795(00)00014-8.
- [10] Siobhán Correnty, Elias Jarlebring, and Kirk M. Soodhalter. Preconditioned infinite GMRES for parameterized linear systems. *SIAM J. Sci. Comput.*, pages S120–S141, 2023. doi:10.1137/22M1502380.
- [11] Guillaume Demésy, André Nicolet, Boris Gralak, Christophe Geuzaine, Carmen Campos, and Jose E. Roman. Non-linear eigenvalue problems with GetDP and SLEPc: Eigenmode computations of frequency-dispersive photonic open structures. *Comput. Phys. Commun.*, 257:107509, 2020. doi:10.1016/j.cpc.2020.107509.
- [12] Cedric Effenberger and Daniel Kressner. Chebyshev interpolation for nonlinear eigenvalue problems. *BIT*, 52:933–951, 2012. doi:10.1007/s10543-012-0381-5.
- [13] Azeddine Essai. Weighted FOM and GMRES for solving nonsymmetric linear systems. *Numer. Algorithms*, 18(3):277–292, 1998. doi:10.1023/A:1019177600806.
- [14] Andreas Frommer and Uwe Glässner. Restarted GMRES for shifted linear systems. *SIAM J. Sci. Comput.*, 19(1):15–26, 1998. doi:10.1137/S1064827596304563.
- [15] Mauricio Garcia-Vergara, Guillaume Demésy, and Frédéric Zolla. Extracting an accurate model for permittivity from experimental data: hunting complex poles from the real line. *Optics Letters*, 42(6):1145–1148, 2017. doi:10.1364/OL.42.001145.
- [16] Brendan Gavin, Agnieszka Międlar, and Eric Polizzi. FEAST eigensolver for nonlinear eigenvalue problems. *J. Comput. Sci.*, 27:107–117, 2018. doi:10.1016/j.jocs.2018.05.006.
- [17] Anne Greenbaum, Miroslav Rozložník, and Zdenek Strakoš. Numerical behaviour of the modified Gram–Schmidt GMRES implementation. *BIT*, 37(3):706–719, 1997. doi:10.1007/BF02510248.
- [18] Stefan Güttel and Françoise Tisseur. The nonlinear eigenvalue problem. *Acta Numer.*, 26:1–94, 2017. doi:10.1017/S0962492917000034.
- [19] Stefan Güttel, Roel Van Beeumen, Karl Meerbergen, and Wim Michiels. NLEIGS: A class of fully rational Krylov methods for nonlinear eigenvalue problems. *SIAM J. Sci. Comput.*, 36(6):A2842–A2864, 2014. doi:10.1137/130935045.

- [20] Nicholas J. Higham, D. Steven Mackey, Françoise Tisseur, and Seamus D. Garvey. Scaling, sensitivity and stability in the numerical solution of quadratic eigenvalue problems. *Int. J. Numer. Method Engineering*, 73(3):344–360, 2008. doi:10.1002/nme.2076.
- [21] Varun Hiremath and Jose E. Roman. Acoustic modal analysis with heat release fluctuations using nonlinear eigensolvers. *Appl. Math. Comput.*, 458:128249, 2023. doi:10.1016/j.amc.2023.128249.
- [22] Elias Jarlebring and Siobhán Correnty. Infinite GMRES for parameterized linear systems. *SIAM J. Matrix Anal. Appl.*, 43(3):1382–1405, 2022. doi:10.1137/21M1410324.
- [23] Elias Jarlebring, Giampaolo Mele, and Olof Runborg. The waveguide eigenvalue problem and the tensor infinite Arnoldi method. *SIAM J. Sci. Comput.*, 39(3):A1062–A1088, 2017. doi:10.1137/15M1044667.
- [24] Elias Jarlebring, Wim Michiels, and Karl Meerbergen. A linear eigenvalue algorithm for the nonlinear eigenvalue problem. *Numer. Math.*, 122(1):169–195, 2012. doi:10.1007/s00211-012-0453-0.
- [25] Daniel Kressner and Jose E. Roman. Memory-efficient Arnoldi algorithms for linearizations of matrix polynomials in Chebyshev basis. *Numer. Linear Algebra Appl.*, 21(4):569–588, 2014. doi:10.1002/nla.1913.
- [26] Philippe Lalanne, Wei Yan, Alexandre Gras, Christophe Sauvan, J.-P. Hugonin, Mondher Besbes, Guillaume Demésy, M. D. Truong, B. Gralak, F. Zolla, A. Nicolet, F. Binkowski, L. Zschiedrich, S. Burger, J. Zimmerling, R. Remis, P. Urbach, H. T. Liu, and T. Weiss. Quasinormal mode solvers for resonators with dispersive materials. *J. Opt. Soc. Am. A*, 36(4):686–704, 2019. doi:10.1364/JOSAA.36.000686.
- [27] Ding Lu, Yangfeng Su, and Zhaojun Bai. Stability analysis of the two-level orthogonal Arnoldi procedure. *SIAM J. Matrix Anal. Appl.*, 37(1):195–214, 2016. doi:10.1137/151005142.
- [28] Volker Mehrmann and Heinrich Voss. Nonlinear eigenvalue problems: A challenge for modern eigenvalue methods. *GAMM-Mitteilungen*, 27(2):121–152, 2004. doi:10.1002/gamm.201490007.
- [29] Xianshun Ming. Quasinormal mode expansion method for resonators with partial-fraction material dispersion, 2023. arXiv:2312.11048, doi:10.48550/arXiv.2312.11048.
- [30] André Nicolet, Guillaume Demésy, Frédéric Zolla, Carmen Campos, Jose E. Roman, and Christophe Geuzaine. Physically agnostic quasi normal mode expansion in time dispersive structures: From mechanical vibrations to nanophotonic resonances. *Eur. J. Mech. A Solids*, 100:104809, 2023. doi:10.1016/j.euromechsol.2022.104809.
- [31] Eric Polizzi. Density-matrix-based algorithms for solving eigenvalue problems. *Phys. Rev. B*, 79:115112, 2009. doi:10.1103/physrevb.79.115112.
- [32] Tetsuya Sakurai and Hiroshi Sugiura. A projection method for generalized eigenvalue problems using numerical integration. *J. Comput. Appl. Math.*, 159(1):119–128, 2003. doi:10.1016/S0377-0427(03)00565-X.
- [33] Tetsuya Sakurai and Hiroshi Sugiura. CIRRR: a Rayleigh–Ritz type method with contour integral for generalized eigenvalue problems. *Hokkaido Math. J.*, 36(4):745–757, 2007. doi:10.14492/hokmj/1272848031.



- [34] Ping Tak Peter Tang and Eric Polizzi. FEAST as a subspace iteration eigensolver accelerated by approximate spectral projection. *SIAM J. Matrix Anal. Appl.*, 35(2):354–390, 2014. doi:10.1137/13090866X.
- [35] Françoise Tisseur and Nicholas J. Higham. Structured pseudospectra for polynomial eigenvalue problems, with applications. *SIAM J. Matrix Anal. Appl.*, 23(1):187–208, 2001. doi:10.1137/S0895479800371451.
- [36] Lloyd N. Trefethen and J. A. C. Weideman. The exponentially convergent trapezoidal rule. *SIAM Rev.*, 56(3):385–458, 2014. doi:10.1137/130932132.
- [37] Roel Van Beeumen, Karl Meerbergen, and Wim Michiels. A rational Krylov method based on Hermite interpolation for nonlinear eigenvalue problems. *SIAM J. Sci. Comput.*, 35(1):A327–A350, 2013. doi:10.1137/120877556.
- [38] Roel Van Beeumen, Karl Meerbergen, and Wim Michiels. Compact rational Krylov methods for nonlinear eigenvalue problems. *SIAM J. Matrix Anal. Appl.*, 36(2):820–838, 2015. doi:10.1137/140976698.
- [39] Shinnosuke Yokota and Tetsuya Sakurai. A projection method for nonlinear eigenvalue problems using contour integrals. *JSIAM Lett.*, 5:41–44, 2013. doi:10.14495/jsiaml.5.41.
- [40] Yujie Zhang and Yangfeng Su. A memory-efficient model order reduction for time-delay systems. *BIT*, 53:1047–1073, 2013. doi:10.1007/s10543-013-0439-z.